

University of Nevada Reno

Using The Great Basin Observatory for Galactic Photometry of Three Elliptical Galaxies

A thesis submitted in partial fulfillment of the requirements for the degree of Bachelor of
Science in Physics

by

Aditya Sidher

Dr. Melodi Rodrigue, Ph.D., Thesis Advisor

December, 2017

University of Nevada, Reno

We recommend that the thesis

Prepared under our supervision by

Aditya Sidher

entitled

Using the Great Basin Observatory for Galactic Photometry of Three Elliptical Galaxies

Be accepted in partial fulfillment of the

Requirements for the

Physics Major

Melodi Rodrigue, Ph.D., Thesis Advisor

David Bennum, Ph.D., Thesis Reader

December, 2017

Table of contents

Abstract	3
Background Information	5
Photometry	5
Stellar Photometry	5
Galactic Photometry	8
Landolt Stars	10
Galaxies	11
Messier 32	11
NGC 3610	12
NGC 5322	12
Applied Photometry and Data Analysis	13
Removing Instrumental Effects	13
Aperture Photometry	17
Unit Conversion	20
Data Analysis	23
Conclusion	25
References	27
Appendix A	30

Abstract

Galaxies are complex systems that contain information about our universe as a whole. This information can be processed through a means of galactic photometry in which multiple images are taken with photometric filters. These filters include ultraviolet (U), blue (B), visible (V), red (R), and near infrared (I). Using these images analyzed with software such as AstroImageJ (AIJ) and Aperture Photometry Tool (APT), we were able to extract information about the galaxies observed. Image processing was done on the images taken by the Great Basin Observatory for each filtered image. Photometry was done on Messier 32, a dwarf elliptical galaxy giving instrumental magnitude of the system.

A galaxy is a huge collection of gas, dust, and billions of stars and their solar systems. There are many different types of galaxies, such as elliptical, spiral, and irregular. Each galaxies has their own unique characteristics that distinguish them from one another. This project specifically looks at elliptical galaxies, which are more smooth and oval shaped compared to spiral galaxies such as our Milky Way. Elliptical galaxies are the most abundant type of galaxies found in our universe. These galaxies contain older stars and little to no gas leading scientists to think there are no new star formations happening within the galaxy (“Elliptical Galaxy”, 2013).

Background Information

Photometry

Photometry is used by many astronomers today to extract information from stars and galaxies. This information is measured as flux. Flux¹ is light energy per second radiated by a source. This information is captured using a charged coupled device (CCD). These images are then analyzed using software, such as AIJ and APT.

Stellar Photometry

Stellar Photometry or the observation of stars can be observed through a variety of different filters available some of the most popular ground-based

¹ Units of power per unit area, or W m^{-2} .

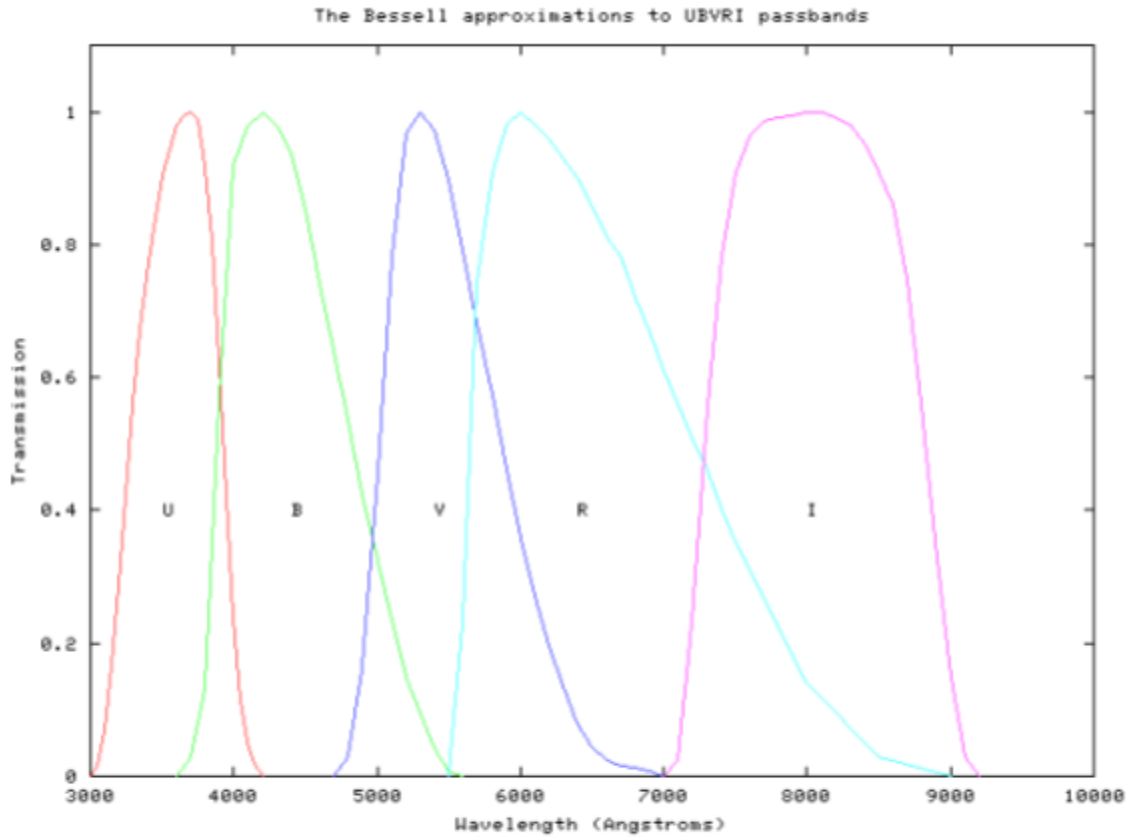


Figure 1.1 Richmond, M. (n.d.). Astronomical spectra, filters, and magnitudes. UBVRI Filters given by Michael Bessell. The Wavelengths respectively for U is between 320-400 nanometers(nm), B is between 400-500 nm, V is between 500-700 nm, R is between 550 - 800 nm, and I is between 700-900 nm.

are the Johnson-Cousins ultraviolet, blue, visible, red, and near infrared (UBVRI) system.

Figure 1.1 shows the wavelength broadband for each filter. These images can then be analyzed further. Such as in stellar photometry where the B-V gives us information on the color index of the star.

By subtracting different images from one another we can find what type of stars we are observing based on its color index (Chromey, 2010, p.333):

$$Index = m(shorter \lambda) - m(longer \lambda) \quad (1)$$

Where m is the monochromatic magnitude and λ is the wavelength. The color index can be used to find the temperature of the system at short wavelengths using Wien's approximation for the surface brightness of a black body (Chromey, 2010, p.334):

$$B(\lambda, T) \approx \left(\frac{2hc^2}{\lambda^5}\right) \exp\left(-\frac{hc}{\lambda kT}\right) \quad (2)$$

Where c is the speed of light in a vacuum, h is Planck's constant, k is Boltzmann's constant, and T is the temperature. At very small temperatures or wavelengths, the index is a linear function (Chromey, 2010, p.334):

$$(m_{\lambda_1} - m_{\lambda_2}) = \frac{a}{T} \left(\frac{1}{\lambda_1} - \frac{1}{\lambda_2}\right) + C(\lambda_1) - C(\lambda_2) \quad (3)$$

Where C is a constant independent of temperature and a source of radius a . Another measurement is the object's apparent magnitude, the magnitude of an object as observed from Earth, and absolute magnitude, the magnitude of an object as seen at a distance of ten parsecs. An object's instrumental apparent magnitude can be measured using the formula:

$$m_{inst} = -2.5 \log(F) + K \quad (4)$$

Where F is the brightness and K is a constant chosen so modern measurements agree (Chromey, 2010, p.27). However for absolute calibration of such a system we need to compare at least one standard star. Thus magnitude difference can be calculated by the equation:

$$\Delta m = m_1 - m_2 = -2.5 \log\left(\frac{F_1}{F_2}\right) \quad (5)$$

Where F_1 and F_2 are both observed flux densities (Chromey, 2010, p.28). It should also be noted that the smaller the magnitude the brighter the flux.

After obtaining the apparent magnitude with photometric calibrations the absolute magnitude can be calculated by:

$$m - M = 5 \log(r) - 5 \quad (6)$$

Where m and M are the apparent and absolute magnitudes and r is the distance to the source in parsecs (Chromey, 2010, p. 28).

Galactic Photometry

Just like stellar photometry, galactic photometry involves using the same methods as before, except instead of measuring a star we measure the surface flux² of the galaxy. We can calculate the galactic surface flux using equation 5.

There are other calculations we can do for galactic photometry such as finding the surface brightness:

$$I(r) = \frac{Flux}{\alpha^2} \sim \frac{Jy}{arcsec^2} \quad (7)$$

Where α is:

$$\alpha = \frac{D}{d} \quad (8)$$

This gives us the surface brightness I(r) which is the amount of light divided by its area in parsec² and where D is the subtended angle for a galaxy at some distance d (“Galaxy Photometry”, 2014, p. 1). Equation 8 can also be related to luminosity where flux is:

$$Flux = \frac{Luminosity}{4\pi d^2} \quad (9)$$

And thus surface brightness becomes:

² Unit of flux density is $\mu Jy/px$ (micro Jansky per pixel).

$$I(r) = \frac{F}{a^2} = \frac{L}{4\pi d^2} \left(\frac{d}{D}\right)^2 = \frac{L}{4\pi D^2} \sim \frac{\text{Watts}}{\text{arcsec}^2} \quad (10)$$

Which is given in solar luminosities per arcsec² (“Galaxy Photometry”, 2014, p.1). The surface brightness can then be converted to magnitudes using equation 5:

$$\mu - \mu_0 = -2.5 \log\left(\frac{I}{I_0}\right) \quad (11)$$

In magnitudes per arcsec² (“Galaxy Photometry”, 2014, p.1).

For calculating the total apparent magnitude of the galaxy we need to integrate over the entire galaxy. This is done through surface profiles based on Sérsic² with “developments by de Vaucouleurs and Petrosian and the exponential case”, this is done in figure 1.2 (“Galaxy Photometry”, 2014, p.2).

The Sérsic Profile

Sérsic Profile (Graham & Driver, Whittle³) describes the intensity of a differential annulus at a distance R from the center of a galaxy:

$$I(r) = I_e e^{-b \left[\left(\frac{r}{R_e} \right)^{1/n} - 1 \right]}$$

where I_e is the intensity in flux per arcsecond² (f/\square^2) at the effective radius R_e enclosing half the total light. The luminosity within some radius, R , is then the integral of this times the area of the differential annulus ($2\pi r dr$) from zero to R :

$$L(R) = \int_0^R 2\pi r I_e e^{-b \left[\left(\frac{r}{R_e} \right)^{1/n} - 1 \right]} dr \quad (1)$$

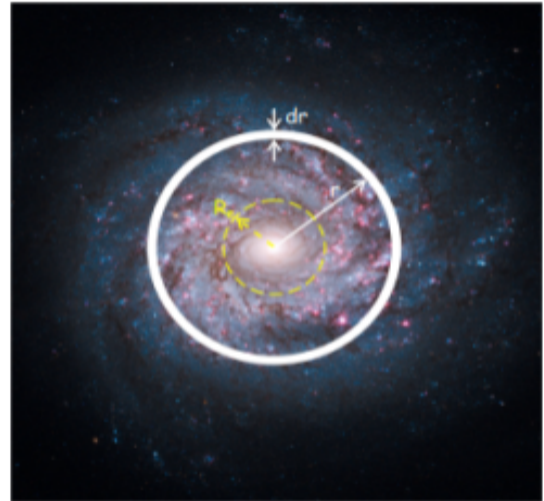


Figure 1.2. “Galaxy Photometry”. (2014). *Sérsic Profile*. Licensed under Undergraduate ALFALFA Team on myslu.stlawu.edu

Landolt Stars

In 1992 and recently in 2013 Dr. Landolt released standard stars, these stars have well characterized magnitudes in each of the photometric filters. Choosing a set of calibration stars known as Landolt Stars help us photometrically calibrate the data.

Name & Distance	RA & DEC	Observable Times (PDT) (Rounded)	Apparent MAG	Type of Galaxy
GD 310 (NGC 3610)	11h 29m 10.9s +38 08m 51.7s	21:00	14.5	White Dwarf
SA 20-245 (M 32)	00h 44m 21.2s +45 55m 12.8s	22:00	8.8	Star
GD 325 (NGC 5322)	13h 36m 01.78s +48 28m 46.2s	21:00	14.0	White Dwarf

Figure 1.3

The standard stars in Figure 1.3 were chosen due their relative nearness to the galaxies being studied. This allows us to calculate a zero point that can then be used with our observed magnitude of the star, giving the true apparent magnitudes of an observed star through the equation:

$$m_{zp} = m_{std} - m_{inststd} \quad (12)$$

Where the m_{std} and $m_{inststd}$ are the catalogued standard star apparent magnitude and its above atmosphere instrumental magnitude of the standard star(Vik Dhillon, 2012). The above atmosphere instrumental magnitude found to be the true apparent magnitude as observed without the Earth's atmosphere. The Landolt standards and their calculated filter/filter subtractions are

given in figure 1.4 below.

Star	V	B-V	V-R	R-I	V-I
GD 310	15.009	-0.178	-0.116	-0.139	-0.250
SA 20-245	8.951	0.866	0.479	0.421	0.894
GD 325	13.968	0.032	0.234	0.776	1.005

Figure 1.4

Galaxies

The galaxies observed by the Great Basin Observatory include two elliptical galaxies and one dwarf elliptical. These galaxies are measured through four filters that include BVRI. The given galaxies are listed in figure 1.5 below.

Name & Distance	RA & DEC	Observable Times (PDT) (Rounded)	Apparent MAG	Angular Size arcmin	Constellation Location	Type of Galaxy
Messier 32 (771 Kpc)	00h 42m 42s +40° 51m 55s	22:00	8.2	3.65 3.18 165 (IR) C	Andromeda	Dwarf Elliptical
NGC 3610 (26.9 Mpc)	11h 18m 25s +58 47m 10.5s	21:00	10.8	1.51 1.09 135 (IR) C	Ursa Major	Elliptical
NGC 5322 (27.1 Mpc)	13h 49m 15.2s +60 11m 25.8s	21:00	10.0	3.54 2.34 87 (IR) C	Ursa Major	Elliptical

Figure 1.5.

Messier 32

Messier 32 is a dwarf elliptical galaxy located near the galaxy Andromeda. It is roughly about 3 billion solar masses and stretches across space 8000 light years in diameter, small

compared to the Milky Way galaxy diameter of 100,000 l.y. M 32 is home to mainly mature red and yellow stars and not much dust and gas can be found. It is believed the Andromeda Galaxy M 31 has ripped off M 32's spiral arms (Plotner, 2017). It was first discovered by Guillaume Le Gentil on October 29th 1749 (Plotner, 2017). A supernova was detected on August 31st, 1998 by a team of astronomers from the University of California at Berkeley ("Messier Objects", 2015). See the Appendix A for observing plan for M32.

NGC 3610

A relatively young elliptical galaxy with a disk still somewhat visible. This galaxy is believed to be a merger of disk galaxies due to its much more disordered appearance, which results from the merging of two or more disc galaxies (Schmidt, 2015). First discovered by William Herchel in 1793 and was later found to contain a disc (Schmidt, 2015). NGC 3610 also has a "rich fine structure" and "warped disk" which is assumed to have originated from previous merges (Schmidt, 2015). See the Appendix A for observing plan for NGC 3610.

NGC 5322

This Elliptical galaxy lies around the Ursa Major constellation. It is considered an irregular round elliptical galaxy with a supermassive black hole of nearly 100 million solar masses (Nooy, 2007). At a conference in Albuquerque, scientists presented the first evidence of a possible origin for the highest-energy variant. A team led by Elihu Boldt at NASA's Goddard Space Flight Center found five High energy cosmic rays from NGC 5322 and NGC 3610 (Wanjek, 2004). See the Appendix A for observing plan for NGC 5322.

Applied Photometry and Data Analysis

Image processing is necessary in order to correctly reduce the amount of photometric data. The steps involved include, removing instrumental effects: including bias subtraction, dark subtraction, flat division, and image correction; digital aperture or area photometry: which will measure the instrumental magnitude inside the atmosphere, m_p^A ; transforming instrumental magnitudes and indices to a standard system: using Landolt stars, m_p^{STD} (Chromey, 2010, p.349). All of this is done through the software AIJ and APT.

Removing Instrumental Effects

It is necessary to do data reduction on our images to permit data analysis and interpretation. The three different effects removed from the images are, bias, dark, and flat.

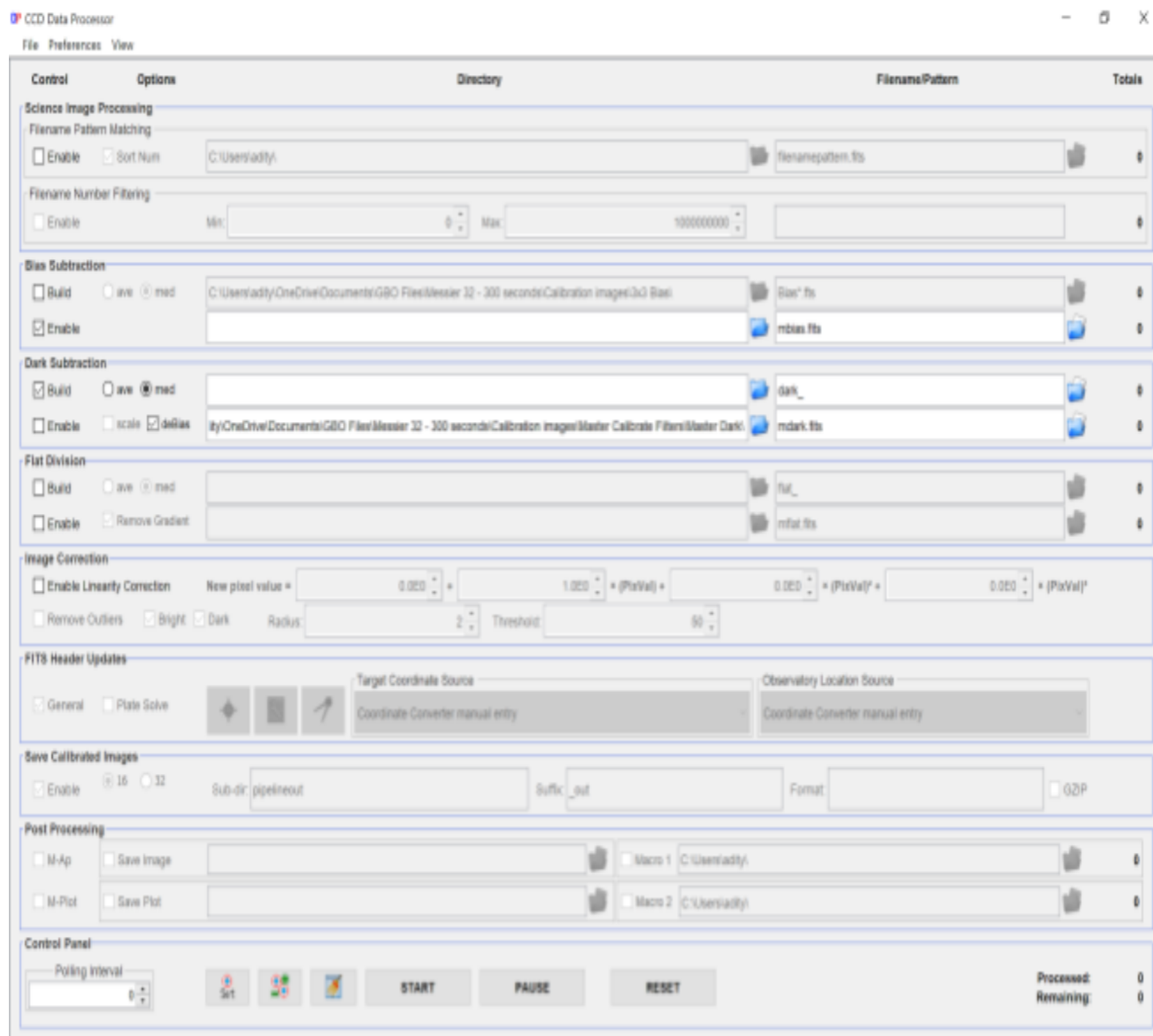


Figure 1.6.

This can all be done in AIJ in the CCD Data Processor plugin under Plugins → Astronomy which is shown in figure 1.6.

A bias frame represents the electronic background present in every frame, no matter how short the integration time, never exposing it to light (Chromey, 2010, p.288).

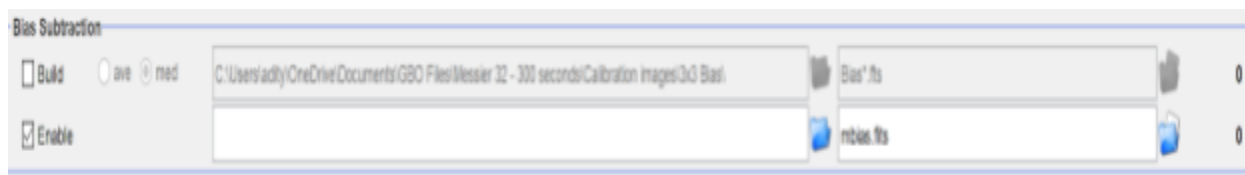


Figure 1.7

By having multiple bias frames we are able to create a master bias frame, or mbias, from the CCD Data Processor plugin shown in figure 1.7, this gives a median of all the bias frames, which can then be used for our calibrations.

The next step after obtaining the mbias is to obtain the master dark, or mdark, through the same method as before. The darks are images of the detector not being exposed to a signal from the telescope, and simply sits in the dark for time t , dependent on the exposure time. Because I wasn't able to obtain the exposure time for 300 seconds, I was able to average the exposure time for a mdark exposed for 240 seconds and another mdark exposed for 360 seconds and scaling these two to get a 300 second exposure mdark image.



Figure 1.8

After getting the mdark, bias subtract, this is all conveniently done through the CCD Data Processor plugin under Dark Subtraction on figure 1.8.

Now to obtain the flat field division for every individual filter. The flat image is obtained by taking an image of a perfectly uniform target with the complete observing system: detector, telescope, and any elements like filters or obstructions (Chromey, 2010, p.292). We will now create a master flat, or mflat, for every filter which include BVRI.

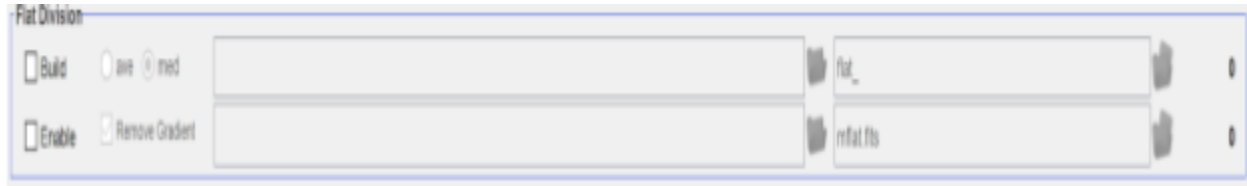


Figure 1.10

All of which can be done through the plugin in figure 1.10.

The last and final part is image processing. This is for calibrating our science frames, such as our observed raw image with the V-band or B-band.

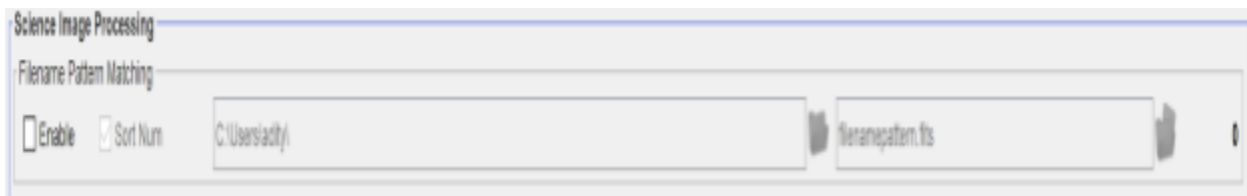


Figure 1.11

This is all done within the Science Image Processing section within the plugin seen in figure 1.11. What this is meant to do is correct the observed raw images by subtracting, the bias, dark, dark scale, and flat division. This gives a calibrated image which can then be used for extracting data.

The calibration is necessary as we can get rid of a lot of outliers within the image that may give errors in the data seen in figure 1.12.

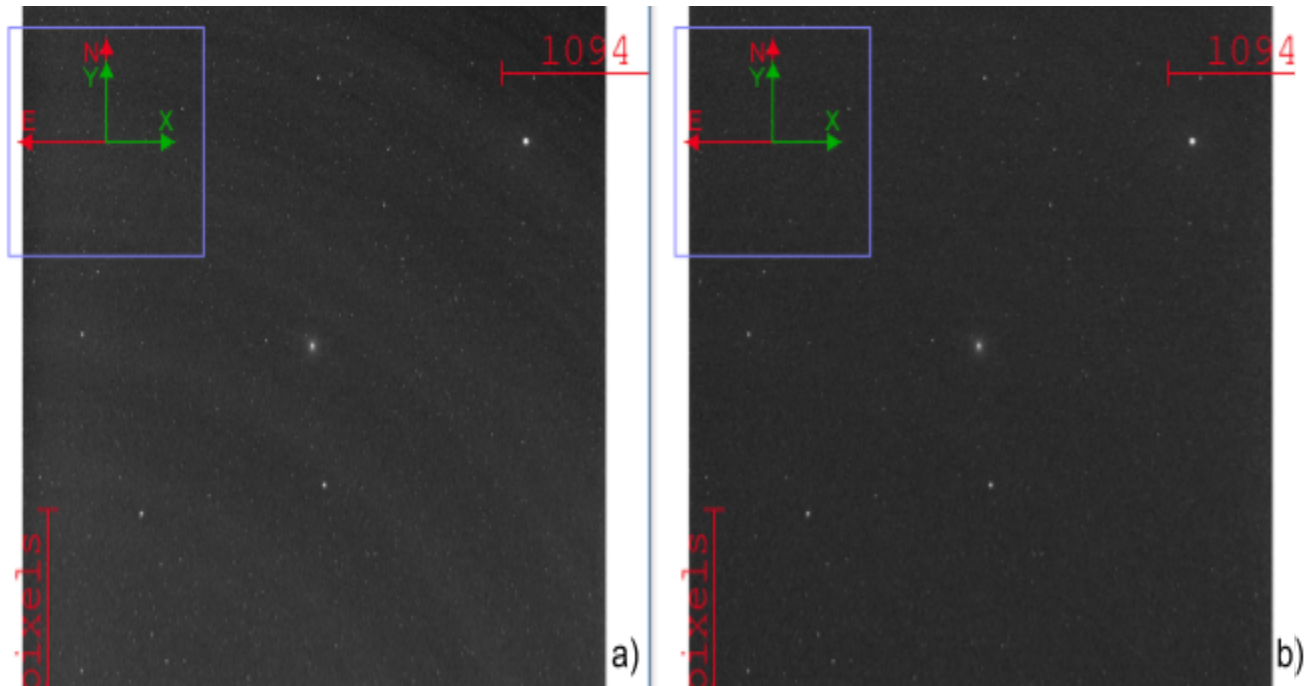


Figure 1.12

Image (a) shows before image processing and image (b) shows after subtraction of mbias, mdark, and mflat division .

Once all of this is done for every science image move onto aperture photometry.

Aperture Photometry

Aperture Photometry is a tool used by astronomers for determining the brightness of a point source, such as a star, quasar, or even galaxies (Chromey, 2010, p.310). In order to do aperture photometry I will use the APT software. Once open we can open the calibrated image from AIJ and by defining a circular area upon the object we are observing, which will be Messier

32, then fix a digital aperture upon our galaxy.

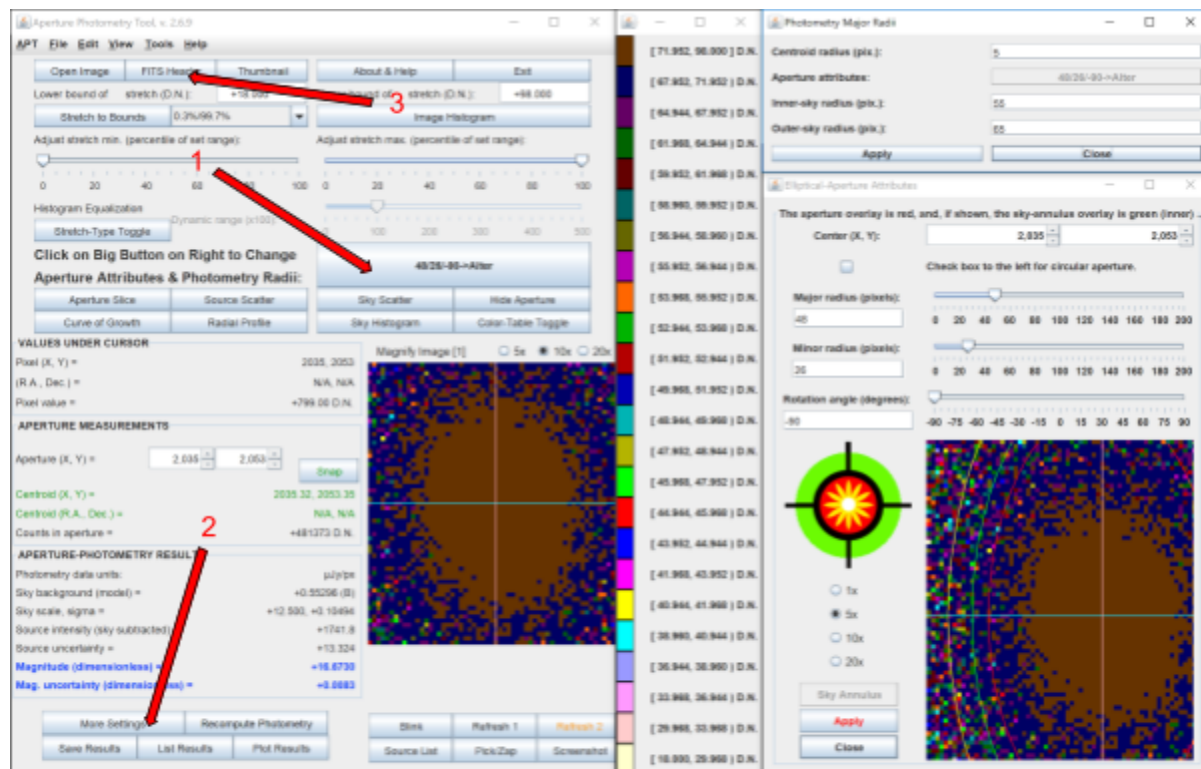


Figure 1.13.

1. Clicking on this will take you to the aperture tool which opens up the Elliptical-Aperture Attributes, and the Photometry Major Radii Windows on the right.
2. This opens up the more settings window which will be used to sky-subtract and correct the pixel count from pixels to $\mu Jy/px$.
3. The FITS HEADER opens up and gives us useful information about our observations.

By clicking on (1) from figure 1.13 open up the aperture placement tool, here place our aperture right on top of M 32 where the pixels are the brightest according to the scale. The more bright pixels are shown on the color table on the middle of the screen going from brightest to dimmest top to bottom. The major and minor radii need to encompass all of the bright pixels. Because M 32 is an elliptical galaxy and has an elliptical shape, using an ellipsoidal shape is used for the aperture shown in figure 1.13 to cover a radius of 48 by 26. Once the centroid radius is fixed, set the inner-sky and outer-sky radii. The inner-sky and outer-sky radii are used for sky-subtraction which helps remove unwanted light from other sources, such as stars or other galaxies

surrounding the object. Once the inner-sky and outer-sky radii are set to 55 and 65 we can hit apply and the software will correctly apply these attributes to the aperture.

The next step is to set an arbitrary constant K, or the instrumental magnitude zeropoint from equation 4, for correcting our magnitude to give us our instrumental magnitude. This is done by clicking (2) from figure 1.13 and opening up the more settings window.

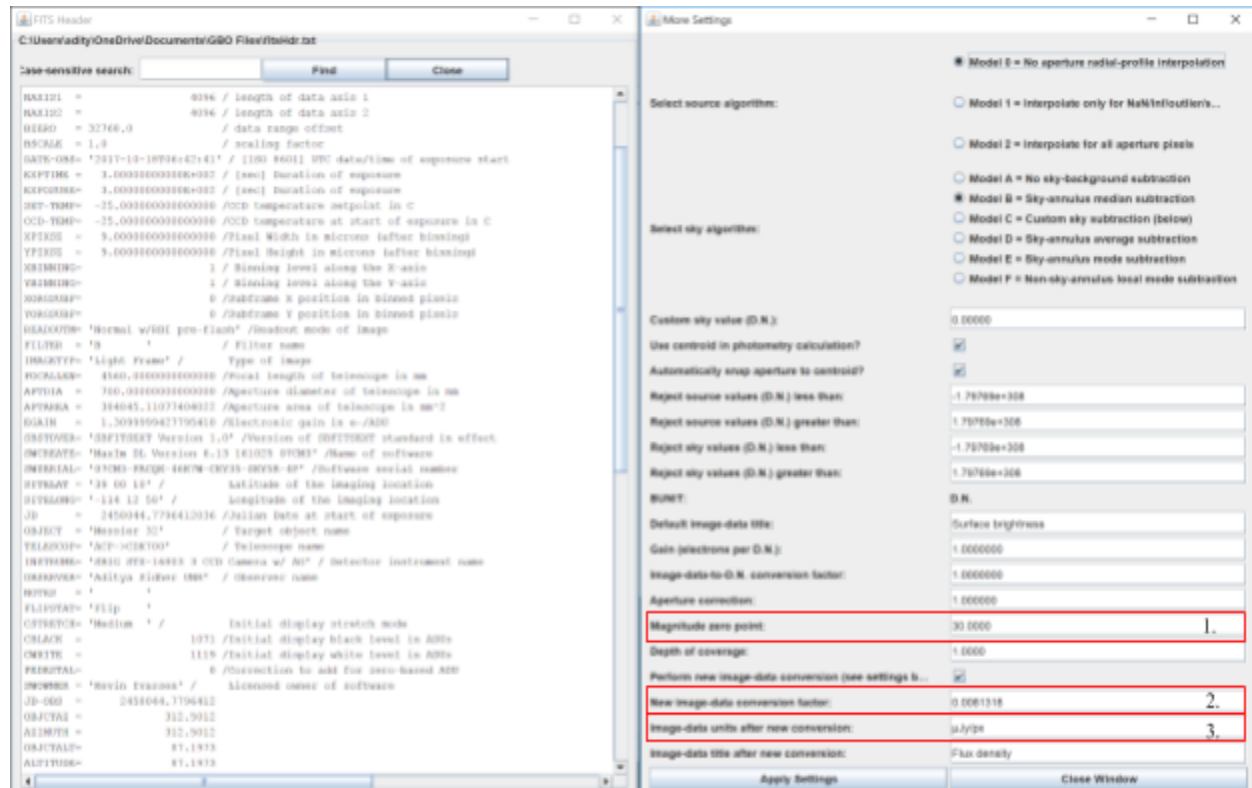


Figure 1.14

1. This is where you input instrumental magnitude, the K zero point constant, set to 30 and will be the same for all other images.
2. This conversion factor is multiplied by the pixel count to give a corrective unit.
3. The units after conversion will be input here as $\mu\text{Jy}/\text{px}$ (micro Jansky per unit pixel).

On (1) in figure 1.14 that the instrumental magnitude zero point will be set to 30 and will be kept the same for all other images. Some other fixes are needed to make the conversions from degree per pixel to micro jansky³ per pixel.

³ Units of Jansky (1 JY = 10^{-26} W/m²/Hz) (“Galaxy Photometry”, 2014, p.1).

Unit Conversion

In order to convert the units, information from our FITS HEADER file is needed, in figure 1.14 (3) on the left. The FITS HEADER file gives information about the telescope and of the observed object. The information needed are all within Appendix B. To convert units the degree per pixel is needed. The degree per pixel is the pixel-distance on CCD pixel arrays and the angle at the sky, or the altitude (Renken & Rath, 1997). Given that it was not provided the equation needed to find it is:

$$\frac{Degree}{Pixel} = \frac{Altitude Degree}{Number of Total Pixels} \quad (13)$$

Where the altitude degree is:

$$Altitude Degree = 90^{\circ} - z \quad (14)$$

The altitude degree is obtained by subtracting 90° from the zenith distance z . The zenith distance is between the observed object and the zenith, the line that goes 90° perpendicular to the surface of the Earth or directly vertical. As shown in figure 1.15 the angle needed,

$$h = 00h\ 53m\ 37.58s - 00h\ 42m\ 41.83s = 00h\ 10m\ 55.75s = 2.73^\circ \quad (17)$$

Now calculate for the zenith distance:

$$z = \sec^{-1} ((\sin(39.003^\circ) \sin(40^\circ) + \cos(39.003^\circ) \cos(40^\circ) \cos(2.73^\circ))^{-1}) = 2.33^\circ \quad (18)$$

With a zenith distance of 2.33° get the altitude degree using equation 14:

$$\text{Altitude Degree} = 90 - 2.33^\circ = 87.67^\circ \quad (19)$$

Now using equation 13 to get:

$$\frac{\text{Degree}}{\text{Pixel}} = \frac{87.67}{4096 \times 4096} = 5.223 \times 10^{-6} \frac{\text{deg}}{\text{px}} \quad (20)$$

There are five steps needed to convert degree per pixel to micro jansky per pixel, step one square the degree per pixel:

$$\frac{\text{Degree}^2}{\text{Pixel}^2} = 5.223 \times 10^{-6} \frac{\text{deg}}{\text{px}} \times 5.223 \times 10^{-6} \frac{\text{deg}}{\text{px}} = 2.7 \times 10^{-11} \frac{\text{deg}^2}{\text{px}^2} \quad (21)$$

Step two convert square degrees to square arcseconds:

$$\left(\frac{60 \text{ arcminutes}}{\text{degree}} \times \frac{60 \text{ arcseconds}}{1 \text{ arcminute}} \right)^2 = \left(\frac{3600 \text{ arcseconds}}{1 \text{ degree}} \right)^2 = 1.296 \times 10^7 \frac{\text{arcsec}^2}{\text{deg}^2} \quad (22)$$

Step three convert arcseconds to steradians, or square radians:

$$\frac{1.296 \times 10^7 \text{ arcsec}^2}{\text{deg}^2} \times \frac{2.3504 \times 10^{-11} \text{ sr}}{1 \text{ arcsec}^2} = 3.046 \times 10^{-4} \frac{\text{sr}}{\text{deg}^2} \quad (23)$$

Step four find the size of the pixels in steradians, combining equations 21 and 23:

$$\frac{2.7 \times 10^{-11} \text{ deg}^2}{\text{px}^2} \times \frac{3.046 \times 10^{-4} \text{ sr}}{\text{deg}^2} = 8.31781 \times 10^{-15} \frac{\text{sr}}{\text{px}} \quad (24)$$

And now lastly step five convert steradians to micro jansky per pixel:

$$\frac{8.31781 \times 10^{-15} \text{ sr}}{\text{px}} \times \frac{1 \times 10^{12} \mu\text{Jy}}{\text{sr}} = 8.31781 \times 10^{-3} \frac{\mu\text{Jy}}{\text{px}} \quad (25)$$

The number from equation 25 was substituted for (2) in figure 1.14 and the units into (3). This scaling will help in the data analysis section.

Data Analysis

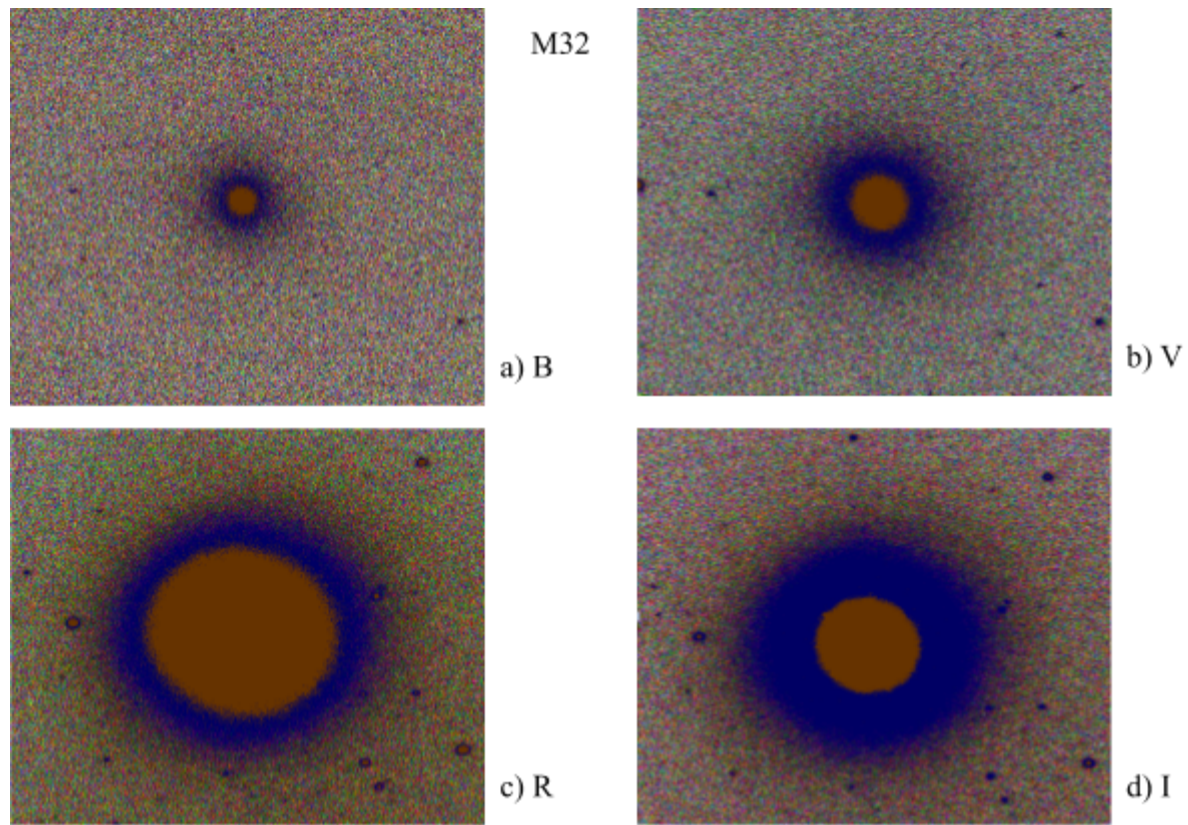


Figure 1.16

- a) Image in the B filter.
- b) Image in the V filter.
- c) Image in the R filter.
- d) Image in the I filter.

Figure 1.16 shows the surface brightness of M 32 within the four different BVRI filters. Because M 32 is a dwarf elliptical galaxy the Red filter (c) already shows the surface brightness being greater than that of the Blue (a), Visible (b), or even the Near-Infrared (d) filtered images.

This is known to be true because elliptical galaxies generally appear to be red. This means that there are stars in the center that are cooler and older. The corresponding instrumental magnitudes are shown in figure 1.17. These correspond to each filtered image which show the surface brightness changing.

Messier 32 Instrumental Magnitudes							
B	V	R	I	B-V	V-R	R-I	V-I
16.3394	14.7855	11.8940	12.2377	1.5539	2.8915	-0.3437	2.5478
+/-	+/-	+/-	+/-	+/-	+/-	+/-	+/-
0.0067	0.0022	0.0010	0.0010	0.0089	0.0032	0.0020	0.0032

Figure 1.17
This table shows the instrumental magnitudes given by APT.

The flux density can be seen through the curve of growth from figure 1.18. Figure 1.18 shows the effective radius of the galaxy which is half of the flux density emitted within the ellipse of

the radius.

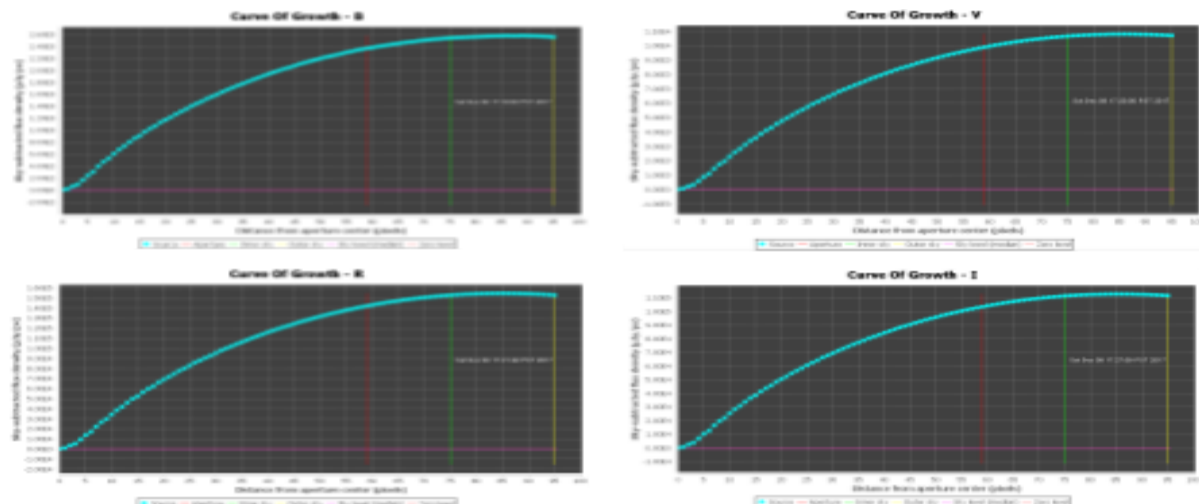


Figure 1.18
The curve of growth BVRI filtered images.

Another thing to notice at the aperture radius, the red vertical line falls before the the peak of the curve. This is due to the constant aperture radius set for each filter, this is done to keep the calibrations the same. Because ground based telescopes were used, changing the aperture won't help that much and keeping the aperture the same all throughout each filter is safer. The curve of growth is plotted with respect to the sky-subtracted flux density vs the distance from the aperture center, or the aperture radius. Unfortunately I was unable to get images for the other two galaxies, NGC 5322 and 3610, and the Landolt stars, GD 310, SA 20-245, and GD 325, so photometry will not be done on these.

Conclusion

Galactic photometry is done by astronomers to measure the surface brightness of galaxies. This is done on a large scale and mostly to search for specific phenomenon within the galaxies. By comparing images taken over long periods of time for each galaxy they may be able to see the changes seen through the magnitude and surface brightness. There are other methods

as well such as galaxy subtraction which will subtract two images of the same galaxy with a gap of six months to see if anything has changed in the galaxy. This is also a common method used in finding supernovae. Because I was unable to get the images from the GBO on my other galaxies and Landolt stars I am not able to do photometry on those objects. There are a few errors that can be observed through this such as the constant kept for the zero point instrumental magnitude, which was set to a constant of 30 to correct each magnitude for each filter. The instrumental zero point is obtained by observing Landolt stars and finding the difference between the instrumental magnitude and the apparent magnitudes observed by Landolt given in figure 1.4. The instrumental zero point cannot be calculated because of the inability to take observations of the Landolt standards due to complications with the telescope.

References

- ALFALFA TEAM. (2016, June 28). *Galaxy Photometry*. Canton, New York, United States.
- Retrieved from
- <http://myslu.stlawu.edu/~aodo/astronomy/ALFALFA/Astronomy%20Basics/GalaxyPhotometry.pdf>
- Case, J. (2017, August 5). *The Relationship Between Altitude and Zenith Distance*. Retrieved from Astro Navigation Demystified:
- https://astronavigationdemystified.com/astronomy_for_astro__cover_for_kindlecolour/
- Chromey, F. R. (2010). *To Measure the Sky*. Cambridge: Cambridge University Press.
- Dhillon, V. (2012, November 26). *Calibrating photometric data*. Retrieved from vikhhillon:
- http://www.vikdhillon.staff.shef.ac.uk/teaching/phy217/instruments/phy217_inst_photcal.html
- Landolt, A. U. (2013). U BV RI PHOTOMETRIC STANDARD STARS AROUND THE SKY AT +50 deg DECLINATION. *The Astronomical Journal*, 9-14. Retrieved from
- <http://iopscience.iop.org/article/10.1088/0004-6256/146/5/131/pdf>
- Messier Objects. (2015, 4 28). *Messier Objects*. Retrieved from messier-objects:
- <http://www.messier-objects.com/messier-32-le-gentil/>
- Nooy, B. D. (2007, March 03). *Astr111 Photography Projects, Spring 2007*. Retrieved from Calvin:
- <https://www.calvin.edu/academic/phys/observatory/images/Astr111.Spring2007/DeNooy.html>
- Palmer, J., & Davenhall, A. (1998, January 29). *The CCD Photometric Calibration Cookbook*.

- Chilton, Oxfordshire, England. Retrieved from
<http://btc.montana.edu/ceres/malcolm/cd/universe/assets/multimedia/sc6.pdf>
- Plotner, T. (2017, January 16). *MESSIER 32 – THE “LE GENTIL” DWARF ELLIPTICAL GALAXY*. Retrieved from universetoday:
<https://www.universetoday.com/33986/messier-32/>
- Renken, H., & Rath, H. (1997). A METHOD FOR THREE-AXIS ATTITUDE DETERMINATION BY IMAGE-PROCESSED STAR CONSTELLATION MATCHING. Am Fallturm, Bremen, Germany. Retrieved from
<http://www.renken.de/or1997.pdf>
- Richmond, M. (n.d.). *Astronomical spectra, filters, and magnitudes*. Retrieved from spiff:
<http://spiff.rit.edu/classes/phys440/lectures/filters/filters.html>
- Romanishin, W. (2006). *An Introduction to Astronomical Photometry Using CCDs*. Oklahoma: University of Oklahoma. Retrieved from
http://www.physics.csbsju.edu/370/photometry/manuals/OU.edu_CCD_photometry_wrc_cd06.pdf
- Schmidt, J. (2015, November 16). *A young elliptical*. Retrieved from spacetelescope:
<https://www.spacetelescope.org/images/potw1546a/>
- Space.com. (2013, 8 15). *Elliptical Galaxy Facts & Definition*. Retrieved from Space:
<https://www.space.com/22395-elliptical-galaxies.html>
- Thompson, A. (2014, January 27). *What is a Supernova*. Retrieved from Space:
<https://www.space.com/6638-supernova.html>
- Walker, E. N. (n.d.). *CCD Photometry*. Retrieved from britastro:

http://www.britastro.org/vss/ccd_photometry.html

Wanjek, C. (2004, April 6). *Fun Times with Cosmic Rays*. Retrieved from Solar System

Exploration:

<https://solarsystem.nasa.gov/news/2004/04/06/fun-times-with-cosmic-rays>

Appendix A

Observation Plans

Messier 32	
Observation Type:	Photometric and visible imaging
Date Range:	14 th and 24 th of every month, September-December
Time Range:	First half of evening (10-12 pm)
Filters Required:	Visible: Clear Focusing Filter, RGB color corrector Photometric: BVR filter
Calibration Frames Required:	Flat Field, Darks
Exposure Time:	300 Seconds

NGC 3610	
Observation Type:	Photometric and visible imaging
Date Range:	14 th and 24 th of every month, September-December
Time Range:	First half of evening (9-12 pm)
Filters Required:	Visible: Clear Focusing Filter, RGB color corrector Photometric: BVR filter
Calibration Frames Required:	Flat Field, Darks
Exposure Time:	300 Seconds

NGC 5322	
Observation Type:	Photometric and visible imaging
Date Range:	14 th and 24 th of every month, September-December
Time Range:	First half of evening (9-12 pm)
Filters Required:	Visible: Clear Focusing Filter, RGB color corrector Photometric: BVR filter
Calibration Frames Required:	Flat Field, Darks
Exposure Time:	300 Seconds

SA 20-245	
Observation Type:	Photometric and visible imaging
Date Range:	14 th and 24 th of every month, September-December
Time Range:	First half of evening (9-12 pm)
Filters Required:	Visible: Clear Focusing Filter, RGB color corrector Photometric: BVR filter
Calibration Frames Required:	Flat Field, Darks
Exposure Time:	15 Seconds

GD 310	
Observation Type:	Photometric and visible imaging
Date Range:	14 th and 24 th of every month, September-December
Time Range:	First half of evening (9-12 pm)
Filters Required:	Visible: Clear Focusing Filter, RGB color corrector Photometric: BVR filter
Calibration Frames Required:	Flat Field, Darks
Exposure Time:	30 Seconds

GD 325	
Observation Type:	Photometric and visible imaging
Date Range:	14 th and 24 th of every month, September-December
Time Range:	First half of evening (9-12 pm)
Filters Required:	Visible: Clear Focusing Filter, RGB color corrector Photometric: BVR filter
Calibration Frames Required:	Flat Field, Darks
Exposure Time:	30 Seconds

Appendix B

Information from FITS HEADER

FITS HEADER	
GBO SBIG CCD Camera Model: STX-16803	
CCD Pixel Size:	9 μm
Focal Length:	4566 mm
Total # of Pixels:	4096 x 4096 = 16777216 pixels
Latitude of Observation (degrees):	39.003°
Declination of the Object Observed:	40°
Right Ascension:	00h 42m 41.83s
Sidereal Local Time:	00h 53m 37.58s